Journal of Dentistry 163 (2025) 106181

Contents lists available at ScienceDirect

Journal of Dentistry

journal homepage: www.elsevier.com/locate/jdent

Influence of test velocity and viscoelasticity on the outcome of the 3-point bending test in modern dental polymer-based composites

Nicoleta Ilie

Department of Conservative Dentistry, University Hospital, Ludwig-Maximilians-University, Goethestr. 70, D-80336 Munich, Germany

ARTICLE INFO

Keywords:
Flexural strength
Crosshead speed
Modulus of elasticity
Dental composites
Mirror constant
Fractography
Dynamic mechanical analysis

ABSTRACT

Objectives: Polymer-based dental composites are considered brittle materials due to their very high filler content. At the same time, the polymer matrix itself and the complex interface between the reinforcing fillers and the polymer matrix induce pronounced viscoelastic behavior. The aim of the study was to relate the variations in the outcome of a 3-point bending test at different crosshead speeds to the viscoelastic material behavior, reliability, and an inherent parameter determined by quantitative fractography.
Methods: A series of three-point bending tests were conducted at crosshead speeds ranging from 0.05 mm/min to 10 mm/min. Variations in strength, elastic modulus, beam deflection and mechanical work were determined for 200 specimens (n = 20) and five crosshead speeds in two different composites. Quantitative and qualitative fractography were used to determine the fracture type and origin. The mirror constant was calculated using the Orr equation. Viscoelastic behaviour was determined using dynamic mechanical analysis (DMA) on frequencies covering human masticatory activity. One and multiple-way analysis of variance (ANOVA), Tukey honestly significant difference (HSD) post-hoc tests (α=0.05) were applied.
Results: Crosshead speed influences the flexural strength significantly. Sensitivity and extent of variation depend on the viscoelastic behavior and are more distinct in materials with pronounced viscoelastic behavior. Elastic modulus, reliability, and mirror constant are speed-independent.
Conclusions: The results highlight the limitations of purely quasi-static tests and underscore the need for a more detailed investigation of the mechanical behaviour of composites to include DMA.
Clinical statement: Composites with improved damping behavior, i.e. better adapted to mechanical impacts, combined with high mechanical parameters, would be preferable for better adaptation to clinical situations.

1. Introduction

The excellent aesthetic adaptation, minimally invasive application and high survival rates of restorations [1,2] make light-curing polymer-based composites (composites) the most popular and frequently used restorative materials worldwide. Their decades of use [3] now enable to assess performance not only based on the survival rate in clinical service, but also to differentiate the individual reason for failure. In this context, secondary caries and fractures were long cited as the main reasons for clinical failure. In recent decades, however, this reason has shifted predominantly to bulk fractures, which account for approximately 70 % of filling replacement cases [2]. Fractures are related to the mechanical behaviour of a composite. The increasingly smaller filler sizes and quantities in modern composites, which are required to improve aesthetics and polishability [4], impair the mechanical properties. This fact must be complemented by the observation that the indication for composite restorations has increasingly expanded to include larger, more complex and multi-surface cavities, where the risk of tooth and restoration fractures is greater [1,2].

Dental composites are considered brittle materials due to their high filler content. However, they show also a pronounced viscoelastic behaviour [5], which is expressed in a strong dependence of the mechanical behaviour on the deformation rate. Viscoelasticity implies behaviour similar to that of both a viscous fluid, where the rate of deformation is proportional to the applied force, and that of a purely elastic solid, where the deformation is proportional to the applied force. In viscous materials, all the work done in the system is dissipated [6], whereas in elastic systems all the work is stored as potential energy. The high complexity of composite materials complicates the development of suitable test methods. Therefore, it is not surprising that most tests focus on static mechanical properties at various scales, neglecting the more complex test methods that consider viscoelastic behaviour. In addition

E-mail address: nicoleta.ilie@med.uni-muenchen.de.

https://doi.org/10.1016/j.jdent.2025.106181
Received 31 July 2025; Received in revised form 10 October 2025; Accepted 14 October 2025
Available online 15 October 2025

to the polymer matrix, the viscoelasticity of a dental composite [5] also depends on its microstructure and the complex interface between filler and matrix, since energy can be dissipated at these interfaces through friction [6]. Therefore, filler quantity, type and size play a crucial role [7]. A higher filler quantity or lower size leads to a larger ratio of the filler-matrix interface where energy can be dissipated, enhancing the viscoelastic nature of the composite [6].

The bending test is by far the most widespread and frequently used test for characterizing the mechanical behaviour of dental composites [8]. Standardization is carried out in ISO 4049 [9], which allows for easy comparison of results from different laboratories. The test result, which is primarily defined by the flexural strength, is considered the most important criterion for material selection [10,11]. In this context, a minimum flexural strength of 80 MPa is defined for composites intended for use in the posterior region [9]. Understandably, this value has been criticized as being too low and, without the additional assessment of the elastic modulus, is considered insufficient for predicting clinical performance [5].

It must be emphasized, that the crosshead speed in the three-point bending test plays a crucial role in determining the mechanical properties of a material and is directly related to the strain rate of the test. Increasing the strain rate generally leads to an increase in strength and can decrease ductility. This effect is often significantly stronger for polymer-based materials whose deformation behaviour exhibits viscoelastic phenomena.

Aware of the limitations of using a simple static test to characterise the mechanical behaviour of composites, the question arises as to what extent the crosshead speed, which may vary even within the specified standard ISO 4049, influences the results. Therefore, the aim of this study was to investigate and quantify the effect of crosshead speed on the outcome of a 3-point bending test using two composites with different filler microstructure and organic matrix composition. The crosshead speed was varied within an interval of 0.05 mm/min to 10 mm/min, thus including the interval of 0.5 mm/min to 1 mm/min specified in the ISO 4049 [9]. In addition, the viscoelastic material parameters were taken into account to relate them to the material behaviour at different crosshead speeds. To achieve this, a clinically relevant aspect was considered when measuring the viscoelastic behavior of the composites. The test was therefore designed to cover human masticatory activity, which occurs at frequencies from 0.94 Hz to 2.17 Hz [12]. The null hypothesis states that the tested crosshead speed in the range of 0.05–10 mm/minute a) has no influence on flexural strength, elastic modulus, mechanical work, beam deflection, reliability, fracture mode or fracture mirror in modern dental composites and b) is independent of differences in viscoelastic behavior.

2. Materials and methods

2.1. Materials

Two representative micro-hybrid, light-cured dental polymer-based composite materials (composites) were selected. Venus (V) is a classic blend of Bis-GMA (bisphenol A-glycidyl methacrylate) and TEGDMA (triethylene glycol dimethacrylate), while Charisma Topaz (CT) is a Bis-GMA free, urethane-based dimethacrylate. The amount of filler and its chemical composition are comparable in both materials, with the exception that CT additionally contains a small proportion of pre-polymerized fillers. Details on the composition and material characteristics are summarised in Table 1.

2.2. Three-point bending test

A series of three-point bending tests were carried out at room temperature and different crosshead speeds by using a universal testing machine (Z 2.5 Zwick/Roell). A total of 200 (n = 20) samples were prepared by compressing the composites between two glass plates with polyacetate sheets in between. The plates were separated by a white split polyacetate (POM) mould with internal dimensions of 2 mm × 2 mm × 25 mm as indicated in ISO 4049:2019 [9]. The specimens were light-cured for 20 s, as recommended by the manufacturer, in the high power mode of a blue-violet LED curing device (Bluephase® PowerCure, Ivoclar Vivadent, Schaan, Liechtenstein; irradiance = 1400 mW/cm^2). After demolding and surface finishing, the samples were stored in artificial saliva at 37 °C for 24 h. The samples were then loaded in a three-point bending setup according to ISO 4049:2019 [9] with a distance of 20 mm between the supports in the universal testing machine with five different crosshead speeds of 0.05, 0.1, 0.5, 5 and 10 mm/min. From the recorded force-deflection diagram, numerous parameters were determined and further evaluated. Flexural strength FS was determined as specified in ISO 4049:2019 [9]. The flexural modulus E was calculated from the slope of the linear part of the force-deflection diagram. The beam deflection ε was recorded during the 3-point bending test and the mechanical work W was calculated as an integral of the force-displacement diagram of the three-point bending test. In addition, reliability was calculated from the FS data by using a Weibull model [13].

2.3. Quantitative and qualitative fractography analysis

The cross-section of the fractured specimens failed in the 3-point bending test at different crosshead speeds are analyzed. Each of the 400 halves created by breaking the samples was examined under a stereomicroscope (Stemi 508, Carl Zeiss AG, Oberkochen, Germany). The half with the most pronounced fracture characteristics was then selected for further analysis. The fracture pattern and fracture origin were subsequently determined using qualitative fractography. The samples were placed under the microscope with the tensile zone facing the examiner. To visualize the characteristic fracture patterns, especially the fracture mirror and the fracture origin, vicinal illumination was used to generate a diffuse reflection that is less dependent on the crack configuration than direct illumination [14]. The first signs of noticeable roughness after the relatively smooth mirror surface were used to

Table 1
Analysed composites: brand, abbreviation (code), shade, batch, and filler composition and quantity (weight and volume percent) as provided by the manufacturer (Kulzer GmbH, Hanau, Germany).

Composite	Code	Shade	LOT	Monomer	Filler	
					Composition	wt %/vol %
Venus	V	A1	K010518	Bis-GMA, TEGDMA	Ba-Al-B-F-Si glass, SiO_2 ∅ = 5 nm – 10 µm	78/59
Charisma Topaz	CT	CL	K010028	TCD-urethane UDMA, TEGDMA	Ba-Al-B-F-Si glass SiO_2, PPF ∅ = 5 nm – 5 µm	75/59

Abbreviations: Bis-GMA: bisphenol A-glycidyl methacrylate, TEGDMA: triethylene glycol dimethacrylate, TCD-urethane: tricyclodecane urethane, UDMA: urethane dimethacrylate, SiO_2: Silicon dioxide, PPF: pre-polymerized filler, ∅: particle size, Ba-Al-B-F-Si glass: barium-aluminum-boron-fluorine-silicate glass, wt: weight, vol: volume.

determine the mirror boundaries. All fracture surfaces were photographed with a microscope extension camera (Axiocam 305 color, Carl Zeiss AG, Oberkochen, Germany). The cause of fracture was identified as either a volume defect (below the surface) or a surface defect located at the edges or corners of the specimens.

The radius of the fracture mirror was then measured in the direction of constant stress, parallel to the tensile side of the specimen, from the fracture origin to the mirror boundary. If the fracture origin could not be precisely determined, the diameter of the mirror was measured and then halved to determine the corresponding radius. The radius was measured using ImageJ version 1.53k software (U.S. National Institutes of Health, Bethesda, MD, USA) and subsequently used to calculate the mirror constant A using the Orr equation described below [14].

$$\sigma\sqrt{R} = A$$

With σ = measured flexural strength; R = radius of the fracture mirror, and A = mirror constant

The strength values σ were therefore plotted against the inverse of the square root of the radius ($1/\sqrt{R}$), with the slope of the line then representing the mirror constant A. The mirror constant A is given for each material and each crosshead speed with its 95 % confidence interval.

2.4. Dynamic mechanical analysis (DMA)

Samples measuring 2 mm × 2 mm × 9 mm ($n = 6$) were prepared for both materials in white acetate molds and polymerized analogously to the samples prepared for the 3-point bending test. After 24 h of storage in artificial saliva at 37 °C, the samples were wet ground with silicon carbide paper (p1200, p2500, and p4000 grit, LECO Corporation, USA) and polished with a diamond suspension (average grain size: 1 μm) for 2–3 min until the surface was shiny (EXAKT 400CS Micro Grinding System automatic grinder, EXAKT Technologies Inc., OK, USA). Measurements were performed by using an automated micro-indenter (Fischerscope® HM2000, Helmut Fischer, Sindelfingen, Germany) equipped with a Vickers diamond tip [15]. For the DMA analysis, a low-magnitude oscillating force was superimposed on a quasi-static force of 1000 mN and applied at 10 different frequencies: 0.5 Hz; 0.7 Hz; 0.9 Hz; 1.1 Hz; 1.4 Hz; 1.8 Hz; 2.3 Hz; 3.0 Hz; 3.9 Hz; 5.0 Hz. The oscillation amplitude was set to 5 nm so that the sample deformation remained within the linear viscoelastic range. A total of 36 indentations were made per material, with six measurement per sample. Ten measurements were performed for each indentation and each of the 10 frequencies [16].

To calculate the viscoelastic material behaviour, the sinusoidal response signal generated by the force oscillation was decomposed into a real and an imaginary part, which represent the storage modulus (E′) and the loss modulus (E″), respectively. E′ characterizes the elastic behavior of the material and E″ the viscous behavior, where the quotient E″/E′ = tan δ represents the damping capacity of the material. In addition, to characterize both plastic and elastic deformation, the universal hardness (H) was calculated by dividing the test load by the surface area of the indentation under the applied test load.

2.5. Statistical analyses

The normal distribution of the data was confirmed by the Shapiro-Wilk test. A parametric approach was used for further analysis. Flexural strength (FS), flexural modulus (E), beam deflection (ε), mechanical work (W), and mirror constant (A) were compared using single-factor and multifactorial analysis of variance (ANOVA) and Tukey's post-hoc test for significant differences (HSD), with an alpha risk of 5 %. The flexural strength data were additionally evaluated using Weibull analysis. The influence of the material and crosshead speed on the above-mentioned parameters was investigated using multivariate analysis (general linear model). For significant independent factors, the partial eta-squared values (η_P^2) indicate the effect strength on the measured data; the higher the η_P^2, the stronger the effect (SPSS Inc. Version 29.0, Chicago, IL, USA).

3. Results

3.1. Three-point bending test

The flexural strength (FS) of the analyzed materials is presented in Fig. 1 as a function of material and crosshead speed. At all tested crosshead speeds, the differences in FS between the materials were large, with CT clearly showing the highest values.

For CT, one-way ANOVA showed that strength increased with increasing crosshead speed, with the speed of 0.5 mm/min resulting in significantly higher FS values ($p < 0.001$) than the statistically similar group with 0.05 and 0.1 mm/min ($p = 0.354$) and statistically significantly lower ($p < 0.001$) than in the group with 5 and 10 mm/min ($p = 0.223$). The variation is similar for V, except that the statistical analysis only distinguishes between two different groups, with lower values at 0.05 and 0.1 mm/min ($p = 0.859$) when compared to the other three faster crosshead speed values ($p = 0.107$).

The Weibull statistics for the FS data are shown in Fig. 2a, b, and c. Reliability was significantly higher for CT compared to V at all tested crosshead speeds. Within the 95 % confidence interval, reliability was maintained with increased crosshead speed for CT. At the limit of statistical significance, there was a slight tendency for the Weibull parameter to decrease in V.

The results for the elastic modulus calculation are summarized in Fig. 3. Here, too, CT clearly outperforms V, but the differences are smaller compared to the FS data. Within a material the crosshead speed has no statistically significant influence on the elastic modulus ($p < 0.001$).

The mechanical work describes the energy transferred to the specimen by the application of force along the test path. The results are summarized in Fig. 4 and show that significantly higher mechanical work is required to fracture CT specimens compared to V. In CT, mechanical work was statistically significant highest at the lowest speed ($p < 0.001$), followed by 0.1 mm/min and then the statistically similar group with the 3 following higher speeds ($p = 338$). The sequence was identical in V.

The beam deflection results are summarized in Fig. 5 and indicate higher values for CT compared to V within the tested crosshead speed

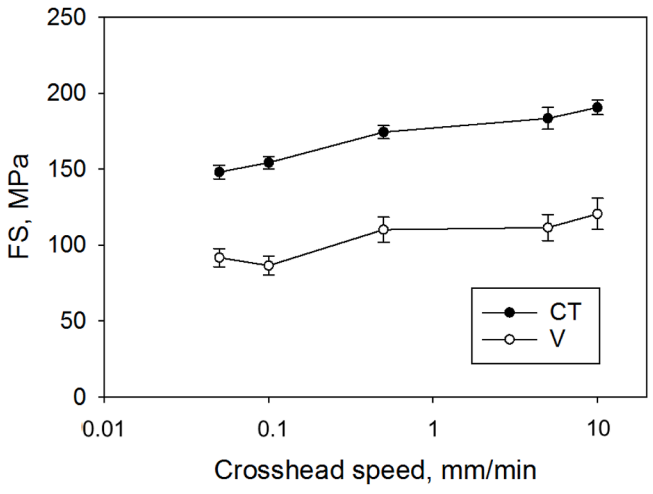

Fig. 1. Flexural strength measured in a 3-point bending test as a function of material and crosshead speed. Data are presented in ascending order of the crosshead speed, which is displayed on a logarithmic scale.

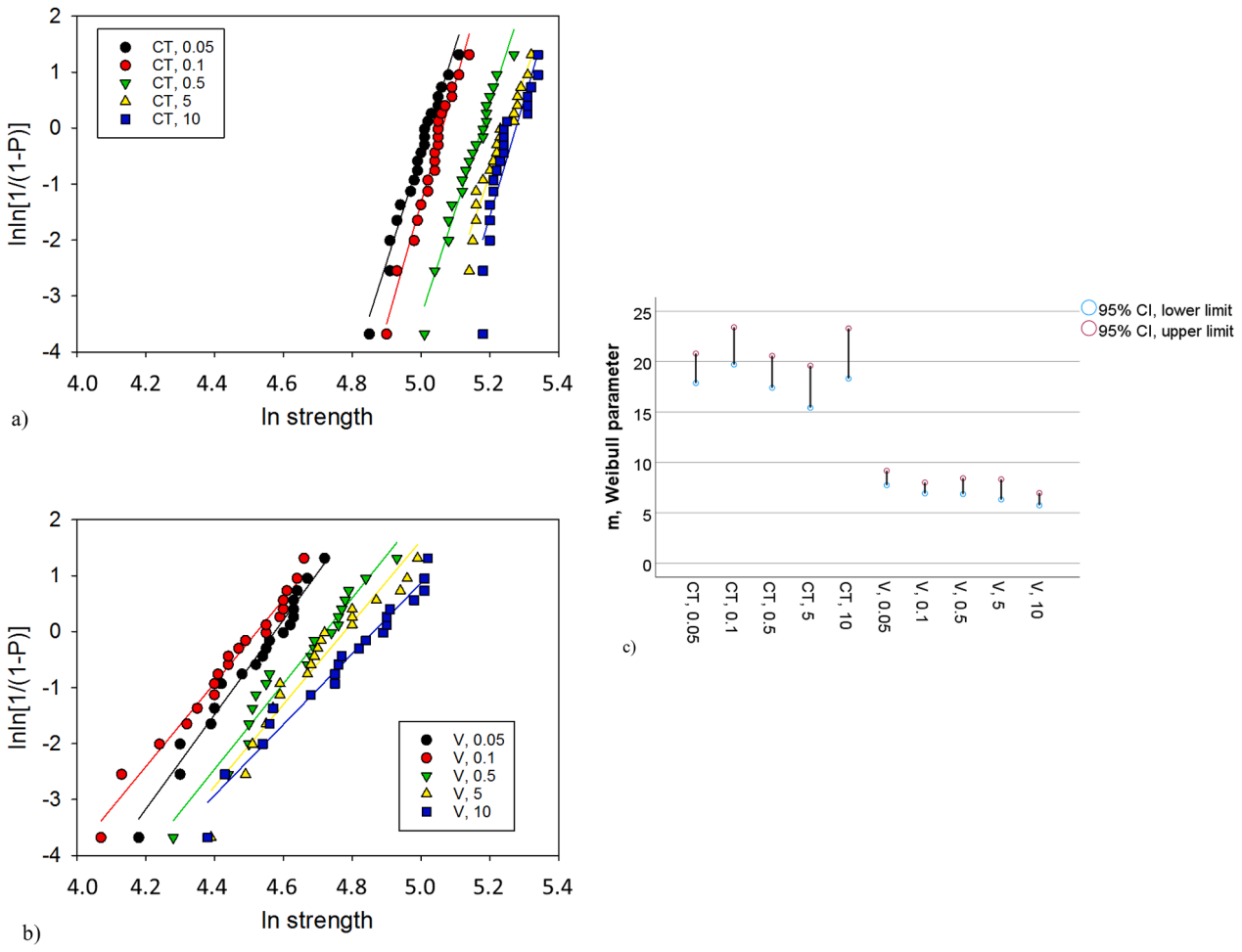

Fig. 2. Weibull plot depicting the empirical cumulative distribution function of strength data. Linear regression was used to numerically evaluate the goodness of fit and estimate the Weibull distribution parameters as a function of crosshead speed in a) CT (Charisma Topaz) and b) V (Venus); c) summary of the resulting Weibull parameter m with the lower and upper limits of the 95 % confidence intervals (CI).

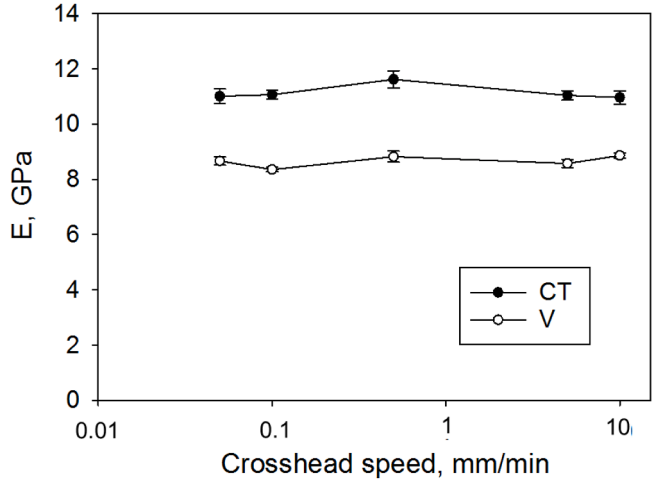

Fig. 3. Flexural modulus measured in a 3-point bending test as a function of material and crosshead speed. Data are presented in ascending order of the crosshead speed, which is displayed on a logarithmic scale.

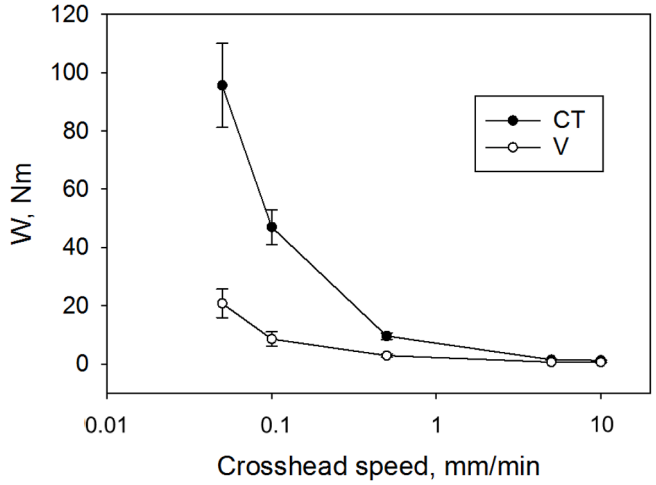

Fig. 4. Mechanical work measured in a 3-point bending test as a function of material and crosshead speed. Data are presented in descending order of mechanical work. The crosshead speed is displayed on a logarithmic scale.

interval. A slight but statistically significant decrease ($p < 0.001$) was observed for CT with increasing speed (0.05 and 0.1 > 0.5, 5 and 10 mm/min), while the differences for V were not statistically significant.

Fig. 6a and b summarize the strength-deflection diagrams for both measured materials as a function of the crosshead speed. The diagrams show a pronounced initial linear dependence for both materials and all crosshead speeds, with deflection increasing at low force, followed by a plastic deformation component with subsequent force increase, which is

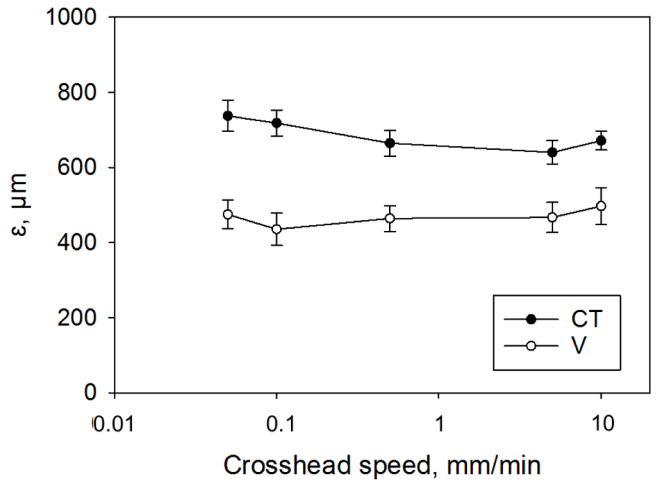

Fig. 5. Beam deflection measured in a 3-point bending test as a function of material and crosshead speed.

more pronounced for CT compared to V. For both materials, at low crosshead speeds, e.g., 0.05 mm/min and 0.1 mm/min, the linear part is followed by a small region where the beam deflection increases at constant stress before plastic deformation. This region begins at higher strength values in CT compared to V. The intermediate region between elastic and plastic deformation is no longer visible at higher crosshead speeds.

3.2. Quantitative and qualitative fractography analysis

3.2.1. Qualitative fractography

All samples fractured in the three-point bending test were analyzed fractographically. Qualitative fractography revealed that volume defects were the predominant defect type (60.3 %) among the 200 specimens fractured in the three-point bending test. Surface defects accounted for 29.9 % (edge) and 7.5 % (corner), while 2.3 % of the defects were not clearly identifiable. Fig. 7 shows the distribution of fracture types within the individual materials and crosshead speeds. The CT shows no clear dependence of the fracture mode on the crosshead speed, while in V the fracture was increasingly triggered by volume defects with increasing

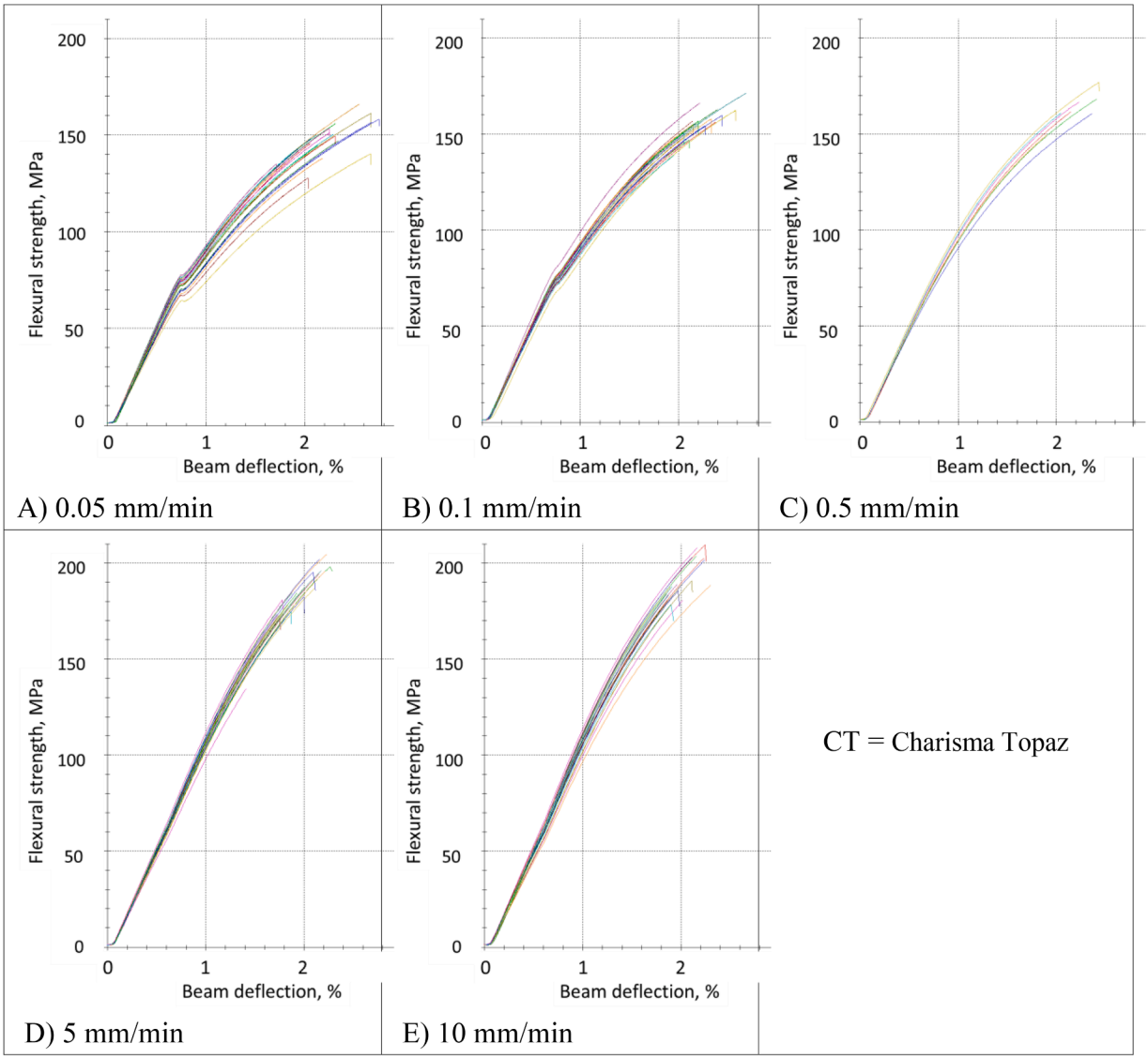

Fig. 6. Force-deflection diagram for the composites a) CT and b) V measured in a 3-point bending test as a function of material and crosshead speed.

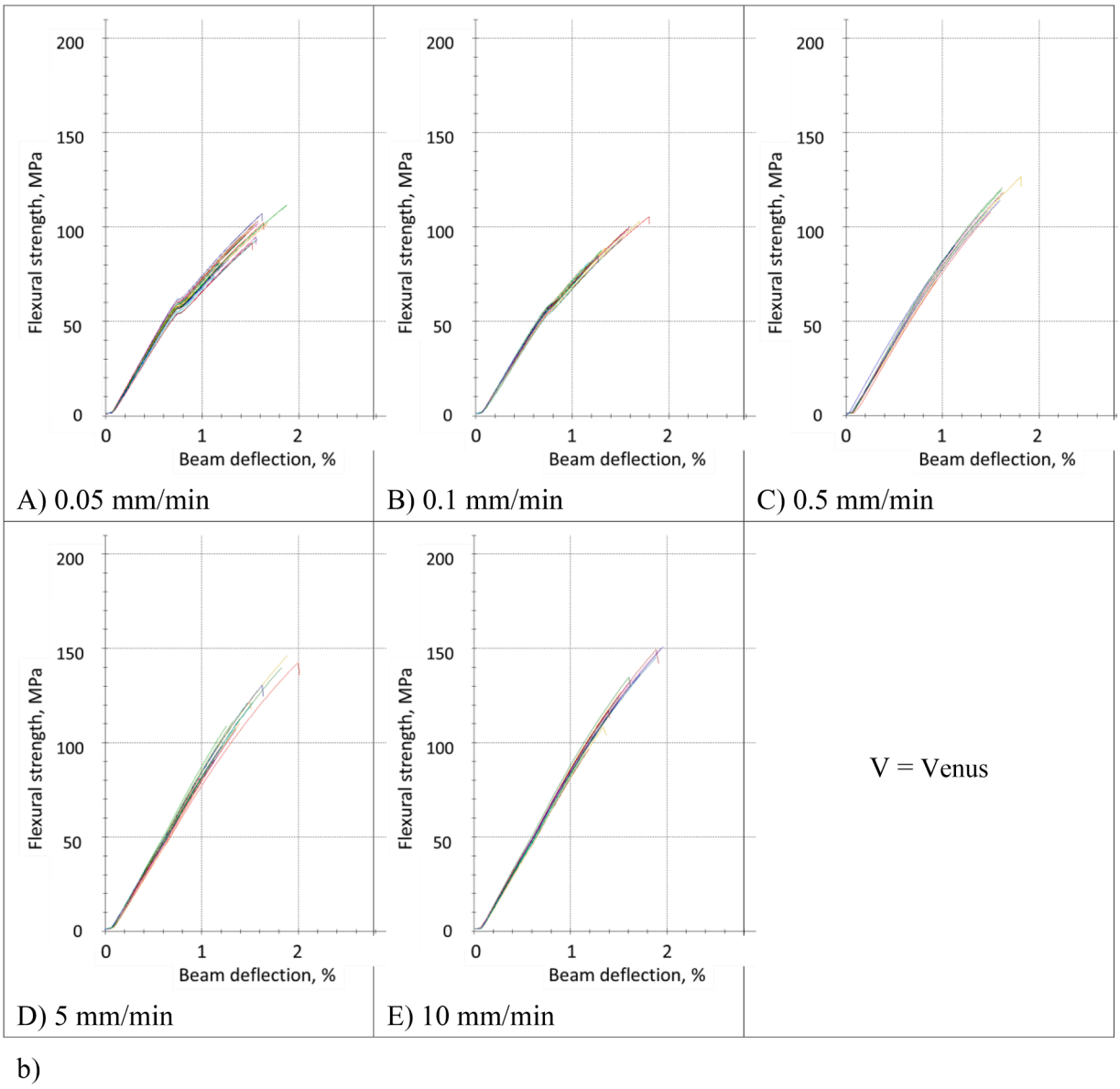

Fig. 6. (*continued*).

crosshead speed.

3.2.2. *Quantitative fractography*

Each specimen fractured in the three-point bending test was examined fractographically to visualize the fracture mirror and measure the mirror radius. The calculated mirror constant A is shown in Fig. 8 and is given with the 95 % confidence interval (lower and upper limits are indicated). The mirror constant was highest in CT comparison to V within the entire crosshead speed interval. In addition, the mirror constant shows a high correlation with the modulus of elasticity (Pearson correlation coefficient = 0.949), flexural strength (0.885), and the beam deflection (0.688).

A multifactorial analysis shows a significant ($p < 0.001$) and strong influence of the material on the measured parameters with the strongest influence exercised on the modulus of elasticity E (higher partial eta-squared value, $\eta_P^2 = 0.887$), followed by flexural strength ($\eta_P^2 = 0.847$), beam deflection ($\eta_P^2 = 0.641$), and mirror radius ($\eta_P^2 = 0.132$). In comparison the effect of crosshead speed was also significant but lower (except for the mirror radius, where the effect was higher), influencing strongest the flexural strength ($\eta_P^2 = 0.493$), then the mirror radius ($\eta_P^2 = 0.232$), the modulus of elasticity E ($\eta_P^2 = 0.123$), and the beam deflection ($\eta_P^2 = 0.052$). The binary effect of material × crosshead speed was low and was statistically significant only for the modulus of elasticity E ($\eta_P^2 = 0.081$) and the beam deflection ($\eta_P^2 = 0.064$).

3.3. *DMA analysis*

The DMA-data is summarised for both materials and the 10 employed frequencies in Fig 9, revealing significant higher values for CT versus V for all parameters and all frequencies. A multifactorial analysis reveals a significant ($p < 0.001$) and high influence of the parameter *material* and *frequency* as well as their interaction product on the measured properties. The effect of the parameter *material* was higher on H_{IT} (η_P^2 =0.619 versus 0.343) and E' (η_P^2 =0.861 versus 0.748). In contrast, the viscoelastic parameters were strongest influenced by the frequency (η_P^2 =0.844 versus 0.568 for E'' and η_P^2 =0.841 versus 0.364 for tan δ).

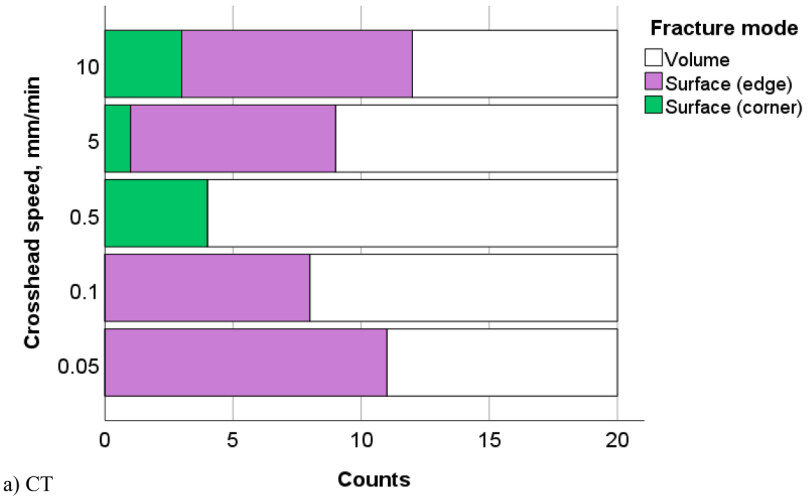

a) CT

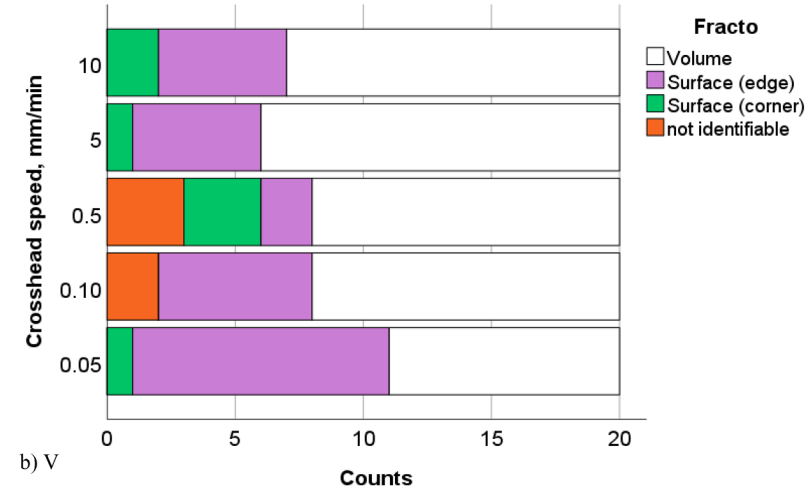

b) V

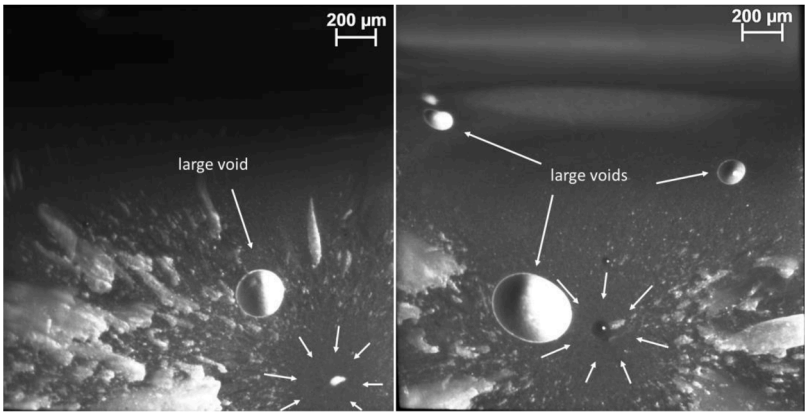

c)

Fig. 7. Fracture mode distribution among analyzed materials as a function of crosshead speed for a) CT (Charisma Topaz) and b) V (Venus); c) Fracture surfaces illustrated for V indicating the occurrence of large voids; small arrows mark the fracture mirror and point towards the fracture origin.

4. Discussion

Developing a suitable test method for complex materials such as polymer-based composites is not an easy task, as their viscoelastic behavior can influence the results to varying degrees. The experimental data confirm that both materials are sensitive to variations in crosshead speed. As the crosshead speed increases, the ultimate strength also increases. This effect was more distinct for the material with the more pronounced viscoelastic behavior, CT. Although a tendency toward an increase in the elastic modulus was also observed, this effect was within the tested speed interval not statistically significant. Furthermore, the beam deflection at failure decreased significantly with increasing crosshead speed for CT, while only a trend was observed for V. It should be mentioned that engineering stress-strain data were used for this calculation because for brittle polymer-based composites, the difference between engineering stress-strain and true stress-strain is generally negligible because yield and failure occur close to each other, resulting in minimal plastic deformation.

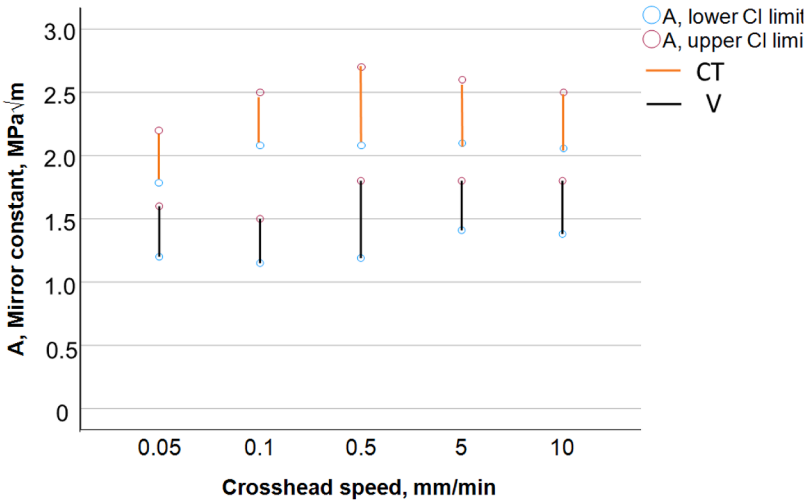

Fig. 8. Mirror constant A calculated from the parameters determined in a 3-point bending test with the 95 % confidence interval (CI) determined for CT (Charisma Topaz) and V (Venus) as a function of crosshead speed.

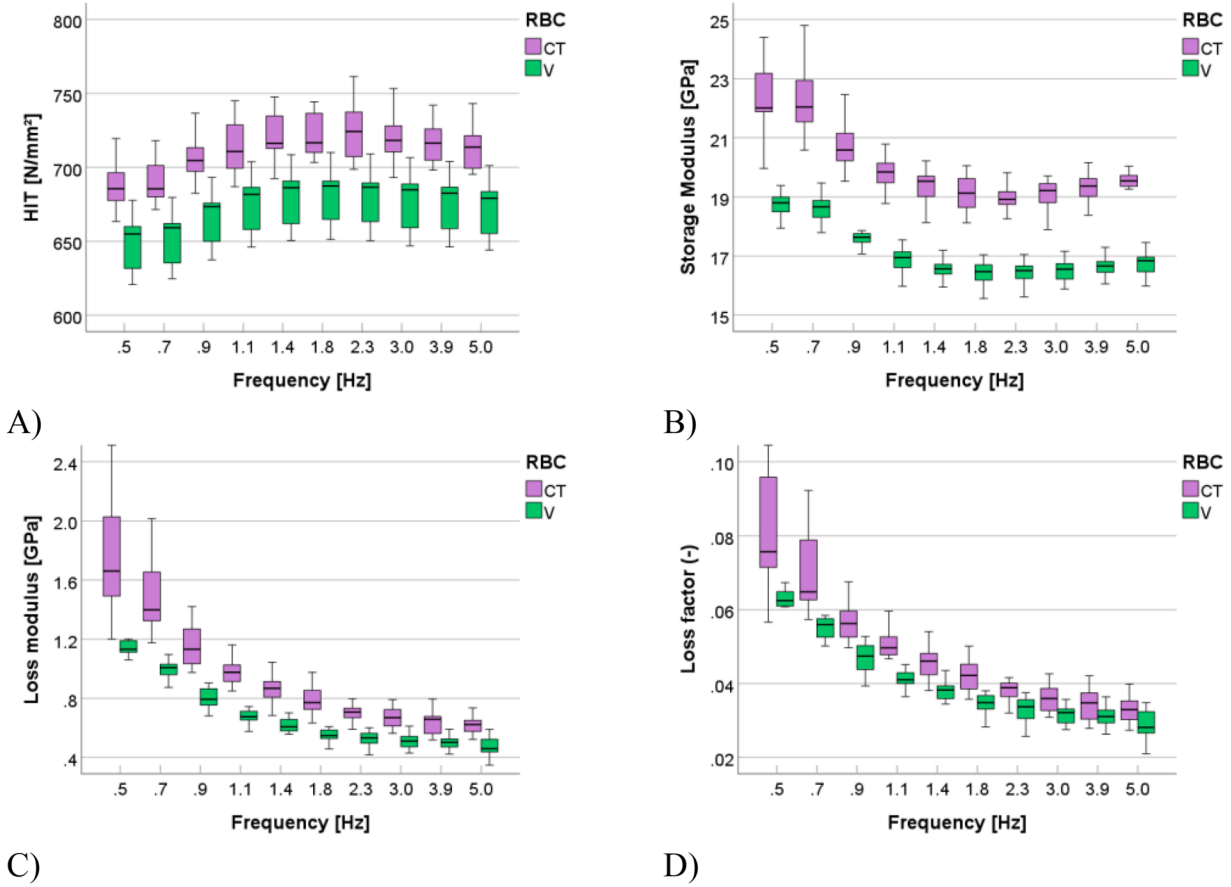

Fig. 9. DMA analysis parameters as a function of material and frequency; A) indentation hardness H_{IT}; B) storage modulus E′; C) loss modulus E″; D) loss factor tan δ.

This behavior needs to be related to microstructural particularities and the viscoelastic material behaviour. The tested materials were quite similar in terms of their filler type, chemical composition and content. Both contain classic Ba-Al-B-F-Si glass fillers and SiO_2 with similar mean sizes and distributions. Manufacturer indicate a slightly lower variation in filler size for CT (5 nm – 5 μm) compared to V (5 nm – 10 μm). The latter is a relevant aspect because the surface treatment is sensitive to the microstructure of the material and the occurrence of surface defects may be related to the filler size and the inherent material roughness. The main difference in the filler system arose from the CT, which additionally contains a small amount of pre-polymerized fillers. The filler amount in volume percent is similar in both materials, but the filler weight is slightly lower in CT, indicating a higher polymer content due to the pre-polymerized filler and consequently a lower inorganic filler amount and a lower modulus. Interestingly, the lower modulus that would result from the above-described conditions could not be confirmed in either the flexural modulus determined in the 3-point bending or the storage modulus determined in the DMA analysis, both

of which were higher in CT than in V. The explanation is found in the composition of the organic matrix, as urethane-based monomer tricyclodecane (TCD) in the organic matrix of CT is more reactive and induces a higher degree of conversion than the bis-GMA (bisphenol A glycol dimethacrylate) / TEGDMA (triethylene glycol dimethacrylate) contained in V [17]. This statement is also supported by data showing that the presence or polyfunctional urethanes [18] in various monomer blends improves the mechanical properties compared to bis-GMA/TEGDMA blends [19].

In addition, consistent with another study [7], a large number of voids were observed in the fracture surfaces of V (Fig 7c), which affects the elastic modulus, as it decreases exponentially with the void fraction [20]. The contribution of voids is less relevant in the DMA analysis, which was performed at shallow indentation depths by visualizing and eluding voids. The lower storage modulus in V observed across the measured frequency range compared to CT in the DMA analysis must also be related to the chemical composition of the polymer matrix and the superiority of poly-functional urethanes in terms of crosslinking and degree of conversion mentioned previously [18].

The presence of large voids/porosities is also clearly reflected in the reliability analysis, which was consistently lower in V compared to CT across the entire range of tested crosshead speeds. The measured strength data for both materials was mathematically well described by Weibull statistics, which was confirmed by the very high R^2 values (>0.90). Interestingly, reliability was maintained at all tested crosshead speeds for both materials however, the nature of the fracture-causing defects appears to vary. For CT, the trend is not as clear, but for V, increased crosshead speed was associated with increased number of volume defects.

Strength-deflection diagrams were used to analyze the crosshead speed impact responses of the composites. At speed values above 0.5 mm/min, only two phases are evident: elastic deformation, characterized by the initial linear part of the diagram, and plastic deformation, characterized by the nonlinear upper part of the diagram. The initially homogeneous elastic behavior is explained by the interaction of the matrix and reinforcement particles under the action of force, and the good adhesion of the particles to the matrix. Elastic deformations in the polymer are caused by the movement of small elements, such as bond length and bond angle, within the polymer chains. The deformation of the polymer at this stage is very small and recoverable. At low speeds, e.g., 0.01 mm/min and 0.05 mm/min, a short transition phase is observed, during which deformation occurs without changes in force. This transition phase (yield phase) observed only at low speeds, is larger for both materials at 0.01 mm/min than at 0.05 mm/min. Yielding is characteristic for the polymer matrix and is a consequence of the molecular uncoiling. It marks the point at which the polymer matrix begins to deform permanently or irreversibly under stress. The yield strength is higher for CT than for V, confirming the improvement of the TCD urethane matrix described above. After yielding, progressive damage of the composite occurs, resulting from matrix deformation, particle detachment, and microcracking, ultimately leading to fracture. Despite the significant similarities in the predominant fillers, there may be differences in the way the materials are damaged under increasing load. These are reflected in the more steeply decreasing stress-strain curve for CT compared to the slightly steeper curve for V in the plastic deformation part. Crack formation in the organic matrix, which begins after yielding at stress peaks, begins to grow along the particle-matrix interface under load. If the particles are sufficiently well embedded, the crack is deflected and consumes more energy. The additional prepolymers in CT act as energy absorbers and can slow down crack propagation, resulting in a higher mirror constant in CT and less brittle behavior compared to V. Furthermore, a certain heterogeneity in the measured data can be caused by inhomogeneous particle distribution, differences in the interfacial adhesion of the particles to the organic matrix, and even microscopic defects such as voids. Since the two materials share many similarities, the latter can be held responsible for the somewhat larger scatter of the measured data in V. The lower crosshead speed is characterized by an exponential increase in mechanical work for both materials, which increased much faster for CT compared to V. This can be attributed to higher energy absorption due to crack deflection, energy dissipation through particle friction, and interfacial failure, which are higher for materials with pre-polymerized fillers and are well related to the viscous parameters—loss modulus (E'') and loss factor ($\tan\delta$)—measured in the DMA analysis. The validity of the 3-point bending measurements and the test setup is confirmed by measuring a steel specimen under identical speed and test conditions, with the force-deflection curves perfectly overlapping at all speeds. The differences in the curve shape of the composites measured at low speed, which evidenced the yield phase, are therefore characterizing a material behavior.

Both composites show significant viscoelastic behavior within the tested frequency range, with an exponential increase in hardness data and a decrease in storage and loss moduli as well as the loss factor ($\tan\delta$) with frequency. The elastic parameters – hardness and storage modulus – are higher for CT than for V, similar to the parameters measured in the macroscopic range, due to the urethane-based polymer matrix discussed above. The interfaces of the pre-polymerized fillers, the slightly higher polymer content and the slightly smaller filler size, which consequently induces an enlarged filler-matrix interface, influence the viscose parameters loss modulus and loss factor in CT, thus enabling a stronger energy dissipation by phase boundary relaxation compared to V. Furthermore, the higher loss factor observed in CT suggests that the material exhibits better damping behavior and shock absorption capacity compared to V, which could clinically imply improved resistance to mechanical impact. This observation is supported by the higher mirror constant observed in CT, which indicates better resistance to crack propagation compared to V. This behavior of having both better elastic and viscous parameters is challenging because the microscopic mechanisms responsible for damping often depend on the parameters controlling mechanical strength. Therefore, CT is a material better adapted to clinical situations compared to V. However, clinical studies have yet to confirm this observation.

Since the tested composites are highly filled, they exhibit a brittle nature that allows the identification of characteristic features in the fracture surfaces: the fracture mirror, i.e., the smooth radial region surrounding the critical flaw that initiated fracture [21], the subsequent mist region formed by secondary cracks that do not further propagate [22], and finally the hackle lines with macroscopic crack branching [23]. The fracture surfaces thus enable the application of quantitative fractography and the calculation of the mirror constant, which can be related to the fracture toughness of the material. While the flexural strength depended on the crosshead speed during the test, the mirror constant was independent for both materials (no overlap of the confidence interval). This result is encouraging, as intrinsic material parameters are needed to characterize mechanical behavior, that are sample size and stress configuration independent.

Based on the investigations conducted in this study, all null hypotheses are rejected.

5. Conclusions

The crosshead speed, in the range of 0.05–10 mm/min, affects the flexural strength in the quasi-static 3-point bending test and the tendency of change depends on the viscoelastic material behavior. It is more distinct in materials with pronounced viscoelastic behavior. In contrast, the modulus of elasticity, reliability and mirror constant are speed-independent.

CRediT authorship contribution statement

Nicoleta Ilie: Writing – review & editing, Writing – original draft, Visualization, Resources, Project administration, Methodology,

Investigation, Funding acquisition, Formal analysis, Data curation, Conceptualization.

Declaration of competing interest

The author declare that she has no known competing financial interests or personal relationships that could have appeared to influence the work reported in this paper.

References

[1] N. Alvanforoush, J. Palamara, R.H. Wong, M.F. Burrow, Comparison between published clinical success of direct resin composite restorations in vital posterior teeth in 1995-2005 and 2006-2016 periods, Aust. Dent. J. 62 (2) (2017) 132–145, https://doi.org/10.1111/adj.12487.

[2] S.D. Heintze, A.D. Loguercio, T.A. Hanzen, A. Reis, V. Rousson, Clinical efficacy of resin-based direct posterior restorations and glass-ionomer restorations - An updated meta-analysis of clinical outcome parameters, Dent. Mater. 38 (5) (2022) e109–e135, https://doi.org/10.1016/j.dental.2021.10.018.

[3] J.L. Ferracane, A historical perspective on dental composite restorative materials, J. Funct. Biomater. 15 (7) (2024), https://doi.org/10.3390/jfb15070173.

[4] S.P. Amaya-Pajares, K. Koi, H. Watanabe, J.B. da Costa, J.L. Ferracane, Development and maintenance of surface gloss of dental composites after polishing and brushing: review of the literature, J. Esthet. Restor. Dent. 34 (1) (2022) 15–41, https://doi.org/10.1111/jerd.12875.

[5] N. Ilie, Cytotoxic, elastic-plastic and viscoelastic behavior of aged, modern resin-based dental composites, Bioengineering 10 (2) (2023) 235.

[6] T.i.-S. Kê, Experimental evidence of the viscous behavior of grain boundaries in metals, Phy. Rev. 71 (8) (1947) 533–546, https://doi.org/10.1103/PhysRev.71.533.

[7] N. Ilie, Microstructural dependence of mechanical properties and their relationship in modern resin-based composite materials, J. Dent. 114 (2021) 103829, https://doi.org/10.1016/j.jdent.2021.103829.

[8] N. Ilie, T.J. Hilton, S.D. Heintze, R. Hickel, D.C. Watts, N. Silikas, J.W. Stansbury, M. Cadenaro, J.L. Ferracane, Academy of Dental Materials guidance-Resin composites: part I-Mechanical properties, Dent. Mater. 33 (8) (2017) 880–894, https://doi.org/10.1016/j.dental.2017.04.013.

[9] ISO, Dentistry — Polymer-based restorative Materials, 4049, ISO/TC 106/SC 1 Filling and restorative materials, 2019, p. 2019.

[10] J.L. Ferracane, Resin-based composite performance: are there some things we can't predict? Dent. Mater. 29 (1) (2013) 51–58, https://doi.org/10.1016/j.dental.2012.06.013.

[11] S.D. Heintze, N. Ilie, R. Hickel, A. Reis, A. Loguercio, V. Rousson, Laboratory mechanical parameters of composite resins and their relation to fractures and wear in clinical trials-A systematic review, Dent. Mater. 33 (3) (2017) e101–e114, https://doi.org/10.1016/j.dental.2016.11.013.

[12] J.M. Po, J.A. Kieser, L.M. Gallo, A.J. Tesenyi, P. Herbison, M. Farella, Time-frequency analysis of chewing activity in the natural environment, J. Dent. Res. 90 (10) (2011) 1206–1210, https://doi.org/10.1177/0022034511416669.

[13] W. Weihull, A statistical distribution function of wide applicability, J. Appl. Mech. 18 (1951) 290–293.

[14] G. Quinn, Guidelines for measuring fracture mirrors, Ceram. Transac. 199 (2007) 163–190, https://doi.org/10.1002/9781118144152.ch14.

[15] ISO, ISO 14577-1, Metallic Materials — Instrumented indentation Test For Hardness and Materials Parameters — Part 1: Test method, 2015, ISO, 2015, p. 46.

[16] N. Ilie, Comparison of modern light-curing hybrid resin-based composites to the tooth structure: static and dynamic mechanical parameters, J. Biomed. Mater. Res. B Appl. Biomater. 110 (9) (2022) 2121–2132, https://doi.org/10.1002/jbm.b.35066.

[17] A. Utterodt, K. Ruppert, M. Schaub, K. Diefenbach, C. Reischl, A. Hohmann, M. Eck, N. Schönhof, in: H.K. GmbH (Ed.), Dental Composites With Tricyclo [5.2.02.6]decane derivatives, European Patent EP1935393, Germany, 2008, p. 3.

[18] N.A. Chowdhury, K. Wakasa, R. Priyawan, M. Yamaki, Dental application of binary urethane monomer mixtures:strengthened resin matrix, J. Mater. Sci. Mater. Med. 8 (3) (1997) 149–155, https://doi.org/10.1023/a:1018571119597.

[19] E. Asmussen, A. Peutzfeldt, Influence of UEDMA BisGMA and TEGDMA on selected mechanical properties of experimental resin composites, Dent. Mater. 14 (1) (1998) 51–56, https://doi.org/10.1016/s0109-5641(98)00009-8.

[20] J.A. Choren, S.M. Heinrich, M.B. Silver-Thorn, Young's modulus and volume porosity relationships for additive manufacturing applications, J. Mater. Sci. 48 (15) (2013) 5103–5112, https://doi.org/10.1007/s10853-013-7237-5.

[21] J. Johnson, D. Holloway, On the shape and size of the fracture zones on glass fracture surfaces, Philosoph. Magaz.: J. Theor. Experimen. Appl. Phys. 14 (130) (1966) 731–743.

[22] E.H. Yoffe, LXXV. The moving griffith crack, Lond., Edinb. Dublin Philosoph. Magaz. J. Sci. 42 (330) (1951) 739–750.

[23] H.P. Kirchner, J. Conway Jr, Criteria for crack branching in cylindrical rods: II, Flexure, J. Am. Ceram. Soc. 70 (6) (1987) 419–425.